



**HAL**  
open science

# Computing the separatrix between dynamic basins of attraction of low dimensional dynamical systems with a time-varying parameter: application to a model of musical instrument

Baptiste Bergeot, Soizic Terrien, Christophe Vergez

## ► To cite this version:

Baptiste Bergeot, Soizic Terrien, Christophe Vergez. Computing the separatrix between dynamic basins of attraction of low dimensional dynamical systems with a time-varying parameter: application to a model of musical instrument. 2023. hal-04378556

**HAL Id: hal-04378556**

**<https://hal.science/hal-04378556>**

Preprint submitted on 8 Jan 2024

**HAL** is a multi-disciplinary open access archive for the deposit and dissemination of scientific research documents, whether they are published or not. The documents may come from teaching and research institutions in France or abroad, or from public or private research centers.

L'archive ouverte pluridisciplinaire **HAL**, est destinée au dépôt et à la diffusion de documents scientifiques de niveau recherche, publiés ou non, émanant des établissements d'enseignement et de recherche français ou étrangers, des laboratoires publics ou privés.

# Computing the separatrix between dynamic basins of attraction of low dimensional dynamical systems with a time-varying parameter: application to a model of musical instrument

Baptiste Bergeot<sup>1\*</sup>, Soizic Terrien and Christophe Vergez<sup>3</sup>

<sup>1</sup>*INSA CVL, Univ. Orléans, Univ. Tours, LaMé EA 7494, F-41034, 3 Rue de la Chocolaterie, CS 23410, 41034 Blois Cedex, France*

<sup>2</sup>*Laboratoire d'Acoustique de l'Université du Mans (LAUM), UMR 6613, Institut d'Acoustique - Graduate School (IA-GS), CNRS, Le Mans Université, France*

<sup>3</sup>*Aix Marseille Univ., CNRS, Centrale Marseille, LMA UMR 7031, Marseille, France*

January 8, 2024

## Abstract

We investigate the behavior of one-dimensional non-autonomous dynamical systems obtained by slowly varying over time the bifurcation parameter of the corresponding autonomous systems, i.e., whose bifurcation parameter is constant. In this context, the study focuses on the case for which the time-varying parameter crosses the bistability domain of the corresponding autonomous system. Considering the time-varying parameter as a new (slow) state variable, the considered non-autonomous one-dimensional system becomes a two-dimensional fast-slow system. In the bistability domain, the latter has attracting manifolds (resp. a repelling manifold) associated with the two stable branches (resp. unstable branch) of the bifurcation diagram of the corresponding autonomous system with constant parameter. In the framework of the geometric singular perturbation theory, we define the separatrix in the phase space between what we call the dynamic basin of attraction of the attracting manifolds. Reverse time numerical integration is used to practically compute this separatrix. Finally the proposed methodology is illustrated on a simple musical reed instrument model. This highlights which asymptotic regime is reached (played note or silence) in the bistability domain, depending on how the musician's control is varied over time.

**Multistability is a common phenomenon in non-linear dynamics. It corresponds to the coexistence, in a dynamical system, of stable solutions for a given set of parameters. A multistable system can switch abruptly from a state to another when a parameter is slightly varied, a phenomenon sometimes referred to as critical transition. In this context, we investigate the behavior of one-dimensional non-autonomous dynamical systems obtained by slowly varying over time a bifurcation parameter of the corresponding autonomous systems, i.e., whose bifurcation parameter is constant. The study focuses on the case for which the time-varying parameter crosses the bistability domain of the correspond-**

**ing autonomous system. Depending on the characteristics of the time-varying parameter, when the bistability domain is crossed, the system can remain close to its current position or leave it abruptly to reach another parameter dependent attractor (called attracting manifold in the paper). Considering the time-varying parameter as another (slow) state variable and then the studied model as a fast-slow system, we define and compute the separatrix in the phase space (which includes the time-varying parameter as another state variable) between what we call the dynamic basin of attraction of a given attractor, i.e., the set of initial conditions leading the system to this attractor. We illustrate our methodology using a simple bistable model of reed musical instrument.**

---

\*Corresponding author: [baptiste.bergeot@insa-cvl.fr](mailto:baptiste.bergeot@insa-cvl.fr)

## 1 Introduction

Nonlinear dynamical systems can possess coexisting stable solutions (or states) for a given set of parameters. This phenomenon is called *multistability* and can imply stable states of different nature such as equilibria, periodic, quasiperiodic and chaotic solutions. To illustrate the concepts considered below we consider the following  $n$ -dimensional autonomous (i.e., with no explicit dependence on time) dynamical system

$$\dot{x} = f(x, \gamma), \quad (1)$$

with  $x \in \mathbb{R}^n$  the vector of state variables,  $\gamma$  the considered control parameter and  $f$  a nonlinear function.

Multistability can be related to the phenomenon of “critical transition”, i.e., a sudden and large change in the output of the system induced by a small change in the input. The link between multistability and critical transition is discussed in the survey article [22] and applications are presented in physics, neuroscience, climate science, biology and ecology. Critical transitions are also referred to as “tipping points”, in particular in climate sciences, and can relate to different phenomena. Ashwin *et al.* [3] propose three categories based on the mathematical description of the underlying mechanisms: *noise-induced transitions*, *bifurcation-induced transitions* and *rate-induced transitions*. Noise-induced transitions, where noise make a multistable system switch from one stable state to another, are not considered in the present article. Then there are the *bifurcation-induced transitions* (or *dynamic bifurcations* [6]) and the *rate-induced transitions*. Both of these transitions consider  $(n + 1)$ -dimensional autonomous systems of the following form

$$\dot{x} = f(x, y), \quad (2a)$$

$$\dot{y} = \epsilon g(y), \quad (2b)$$

associated to Eq. (1) but with a time-varying bifurcation parameter  $y$  which therefore becomes a new state variable. The time variation of the latter is slow compared to the original time scale of Eq. (1); this is accounted for here by the small dimensionless parameter  $\epsilon$  in the right-hand side of Eq. (2b).  $y$  is called the *slow variable*, the variables of the original state vector  $x$  are called the *fast variables* and Eq. (2) is a *fast-slow* dynamical system. Solutions of Eq. (1) (both transient and stationary) are no more solutions of Eq. (2) since  $y$  is no constant in time anymore. However, stable stationary solutions of Eq. (1) are associated with attracting invariant manifolds of Eq. (2) that evolve in its  $(n + 1)$ -dimensional phase space and attract orbits which are in their vicinity [21, 27]. Bifurcation-induced transitions correspond to

the slow variable  $y$  passing through a bifurcation point  $\gamma^*$  at which the considered stable solution of Eq. (1) losses stability. At this point, the corresponding manifold of Eq. (2) ceases to be attracting and in general the transition to another attracting manifold does not appear at  $\gamma^*$  but at a larger value through a phenomenon of *bifurcation delay* [11, 34, 28]. The rate-induced transitions, identified by Wieczorek *et al.* [35], are transitions between stable attracting manifolds of Eq. (2) without the presence of noise or a bifurcation point. In this case the critical transition is only due to the time variation of parameter under consideration. Considering equilibria of Eq. (1) (becoming a one-dimensional manifold of Eq. (2)), Ashwin *et al.* [3] derived the critical value of the parameter  $\epsilon$  above which the orbit of the system leaves the attracting manifold it was going along.

In Ref. [2], Ashwin *et al.* introduce a formalism that uses so-called pullback attractors to describe the phenomena of bifurcation-induced transitions and rate-induced transitions, again considering equilibria. The method is extended by Alkhayoun and Ashwin [1] to the case of stable periodic solutions of Eq. (1), becoming two-dimensional manifolds of Eq. (2). In a realistic physical system, critical transitions may be associated with a combination of the three mechanisms mentioned above.

The works cited in the previous paragraph focus on the conditions causing an orbit to leave the neighborhood of a manifold that it was following. Therefore, these works deal with the beginning of the critical transition. However, the question of the end of the transition, when several other attracting manifolds can be potentially reached, is poorly addressed in the literature. In the case of dynamical system with constant parameters (i.e., of type (1)) for an asymptotically stable solution to be reached, the initial conditions must be in its *basin of attraction*, i.e., the set of initial conditions leading to it. What happens to the notion of basin of attraction when the control (or bifurcation) parameter slowly varies over time, i.e., when Eq. (2) is considered? In other words, what happens to an orbit of Eq. (2) when it leaves the neighborhood of a given attracting manifold (or a manifold which has been locally attracting) and several other attracting manifolds exist?

In this paper, we propose first elements of response to these questions. To do so, (i) we consider a one-dimensional original system (i.e.,  $x \in \mathbb{R}$  in Eq. (1) and (2)) and (ii) we consider the framework of the geometric singular perturbation theory (GSPT) [21, 27] which provides general results on the behavior of fast-slow dynamical systems. In this context, the concepts of *dynamic basin of attraction* (DBA) and of the separatrix between two DBAs are introduced. Basically, these con-

cepts can be exemplified as follows: if, in the case of a one-dimensional nonlinear ODE with a constant control parameter (i.e., of type (1) with  $x \in \mathbb{R}$ ), the system is bistable with two coexisting stable equilibria whose basins of attraction, called here *static basin of attraction* (SBA), are separated by an unstable equilibrium; then, for the same ODE with a slowly time-varying control parameter (i.e., of type (2) with  $x \in \mathbb{R}$ ) the stable equilibria becomes attracting one-dimensional manifolds that evolve in the two-dimensional phase space. Depending on the initial condition considered, one or other of these manifolds is reached by the system orbit. The set of initial conditions, in the two-dimensional phase space, leading to a given attracting manifold constitutes the DBA of this manifold. Logically, the Separatrix Between two DBA (SDBA) also becomes a one-dimensional manifold. The present research aims (i) to propose mathematical definitions of DBA and SDBA and to propose a method to compute the SDBA and (ii) to illustrate the method on a toy model of reed instrument with a linearly time-increasing mouth pressure parameter.

Self-sustained musical instruments - such as wind instruments, bowed string instruments or singing voice - are nonlinear dynamical systems known to produce a diversity of different sound regimes. An important specificity is that sound production in a musical context is associated to a time-varying control. Indeed, control parameters are modified continuously by the instrument player. In particular, wind instruments players control air pressure in their mouth with variations over time finely tuned, first to start the sound and then to obtain the desired sound effect. However, in general, when the corresponding mathematical models of musical instruments are analyzed, the control parameters are assumed to be constant. Consequently, the instruments are modeled by autonomous nonlinear systems of differential equations (ODEs) which can have a wealth of solutions including equilibria, periodic and quasiperiodic solutions. In this context, the silence corresponds to the trivial equilibrium of the instrument model and a musical note to a periodic solution. In general, for a given set of constant control parameters, this desired periodic solution is not the only stable solution of the model. In practice, from the point of view of instrument playing, the size of the SBA of a given periodic solution can be linked to the ease with which the corresponding note can be played. For example, in the case of a reed instrument such as the saxophone, musicians know that for a given fingering corresponding to a low pitch note, the first harmonic of the desired note are sometimes easier to play. It is also on this principle of multistability that brass instruments, such as trumpets, operate.

In physical models of wind musical instruments, state variables are classically the modal pressures and their derivatives: these are the fast variables of Eq. (2). The considered control parameter is the pressure inside the mouth of the musician. We assume that it varies slowly over time and it is considered as another state variable: the slow variable such as  $y$  for Eq. (2). In this context, previous theoretical works by the authors [7, 8, 10] investigated the emergence of oscillations in simple models of reed instruments in which the pressure in the mouth, which is the control parameter, varies over time. This allowed to interpret experimental results [9] as the manifestation of the bifurcation delay phenomenon. After studying this in the case of the appearance of oscillations, we investigate here the influence of the temporal dynamics of the mouth pressure on the nature of the regime reached in the presence of multistability. A problem that has been preliminary studied by Colinot *et al.* [18] through *a posteriori* observations on results of direct time numerical integration of a saxophone model. Authors showed that different regimes may be reached by modifying the mouth pressure dynamics. Here, we focused on the underlying phenomena allowing us to interpret these kinds of observations. Although the dynamics observed in this particular system corresponds to a bifurcation-induced transition, the concepts of BDA and SDBA might also be of interest in the case of rate-induced transitions.

The paper is organized as follows. In Section 2, the single reed instrument model under consideration is briefly presented. The static bifurcation diagram of the model is computed in Section 3. Section 4 provides elements of geometric singular perturbation theory needed for the mathematical definition of the DBA and of the separatrix between two of them. The latter are defined in Section 5.1 in which the method used to compute the separatrix is also presented. The method is then illustrated on the studied model in Section 5.2. A discussion about the case of a blowing pressure which saturates in the bistability domain and about the extension of the method to more realistic models of instruments is proposed in Section 6. Finally, concluding remarks and some perspectives are given in Section 7.

## 2 Background on the physical model of reed instrument

The model of single reed instrument model considered in the paper consists in a classical toy model obtained under strong assumptions (see Section A.1). We focus here on dynamic basins of attraction mentioned above and describe a method to define and compute the separatrix between two basins. For sake of conciseness, details on

the clarinet model (which is classical in musical acoustics) are presented in the Appendix A.

The state variables are the pressure  $p$  at the entrance to the instrument resonator (i.e., inside the mouthpiece) and its first time derivative and the bifurcation parameter is the blowing pressure  $\gamma$ . We consider the averaged dynamics of this model, in which the amplitude  $x$  of  $p$  is a state variable, with a time-varying blowing pressure (the control parameter under consideration in this work), now considered as another state variable and denoted  $y$  (see Section A.2).

Equations of the averaged dynamics are of the form of Eq. (2), i.e.,

$$\dot{x} = f(x, y), \quad (3a)$$

$$\dot{y} = \epsilon g(y), \quad (3b)$$

with  $(x, y) \in \mathbb{R}^2$ . Eq. (3a) is the equation of the physical instrument model and Eq. (3b) describes the time variation of the blowing pressure  $y$ . The function  $f$  is derived from the so-called nonlinear characteristic (NLC) of the instrument exciter which links the volume flow through the reed channel to the pressure difference between the mouth and the mouthpiece and has been widely studied in the literature [26, 19].

In the following sections, we refer to *static* when the mouth pressure is time-constant (i.e.  $\dot{y} = 0$ ) and to *dynamic* when the mouth pressure is time-varying (i.e.  $\dot{y} = \epsilon g(y)$ ).

### 3 Static bifurcation diagram of the model

The *static bifurcation diagram* is a commonly used tool in musical acoustics (see e.g. Refs. [16, 25]). It provides useful information beyond the purely static case, and has shown its interest in the dynamic case, in particular in a model of reed musical instrument [10, 7, 8]. Here, the static bifurcation diagram is computed by stating  $\dot{y} = 0$  with  $y = \text{const.} = \gamma$  in Eq. (3). Fixed points of  $\dot{x} = f(x, \gamma)$  (with  $f$  given by Eq. (36)) are computed by solving  $f(x, \gamma) = 0$ . In practice, we use the function `NSolve` of the Mathematica software [37].

The trivial fixed point is the equilibrium solution of the original (non-averaged) dynamics (27) and the non trivial fixed points correspond to the periodic solution of (27). The stability of the fixed points is determined subsequently from the sign of  $\partial_x f(x, \gamma)$ .

Fig. 1 shows the static bifurcation diagram obtained for the modal parameters of the air-column and the embouchure parameter  $\zeta$  given in Table 1. Unless stated otherwise, the parameter values given in Table 1 are used through out the article. Fig. 1 shows that the model is

**Table 1.** Modal and embouchure parameters. Taken from Ref. [25]. Unless stated otherwise, these parameter values are used through out the article.

Modal parameters	$\epsilon_1 = 1/36.6$ $\omega_1 = 1440$ $Z_1 = 50$
Embouchure parameter	$\zeta = 0.1$

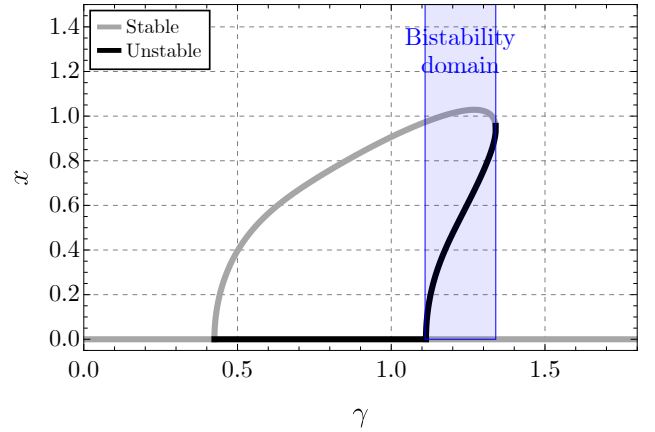


**Figure 1.** Static bifurcation diagram of the clarinet obtained by averaging procedure. A bistability domain is observed between  $\gamma = 1.11$  and  $\gamma = 1.34$  and depicted by an blue colored area. The parameters given in Table 1 are used.

bistable between  $\gamma = 1.11$  and  $\gamma = 1.34$ . Within this range of the parameter value the trivial fixed point and a non trivial fixed point are stable and, lying between them, the other non trivial fixed point is unstable.

For a given stable solution, the *static basin of attraction* (SBA) is the set of initial conditions leading to this solution. Here, for our 1D system  $\dot{x} = f(x, \gamma)$ , the separatrix between the SBAs of the two stable fixed points in the bistability domain is trivial, and is the unstable fixed point.

### 4 Elements of geometric singular perturbation theory

In this section some basics of the geometric singular perturbation theory (GSPT) [27] are recalled. System (3) is considered for sake of illustration. In the GSPT framework (i) the latter is a (1, 1)-fast-slow system, i.e., a dynamical system with one fast variable ( $x$ , here the amplitude of the mouthpiece pressure) and one slow variable (here  $y$ , the blowing pressure) and (ii)  $t$  represents the fast timescale. Most of these elements of GSPT are reproduced from Berglund and Gentz [12, 13] and Kuehn [29].

Eq. (3) is now written on the slow timescale  $\tau = \epsilon t$ , Eq. (3) becomes

$$\epsilon x' = f(x, y) \quad (4a)$$

$$y' = g(y), \quad (4b)$$

where  $\{\}' = d_\tau\{\}$  (the first time derivative with respect to the slow time  $\tau$ ).

As an illustration, Fig. 2 shows an example of possible time series  $x(\tau)$  and  $p(\tau)$  obtained from the numerical integration of the averaged system (4) and of the original system (27) (replacing  $\gamma$  par  $y(t')$  and switching from  $t'$  to  $t$ , see Appendix A), respectively. We considered a linear time variation of the slow variable, i.e.,

$$y(\tau) = \tau + y_0, \quad (5)$$

or  $y(t) = \epsilon t + y_0$ , with  $y_0 = y(0)$ . Therefore, the function  $g(y)$  is simply

$$g(y) = 1. \quad (6)$$

We used the parameters given in Table 1.

The time profile of the linearly increasing blowing pressure  $y(\tau)$  is also represented. Overall, the figure shows an excellent agreement between time series  $x(\tau)$  and  $p(\tau)$  which validates the averaging procedure.

The time evolution of slow-fast systems is characterized by possible successions of fast epochs and slow epochs. This is shown in Fig. 2. Indeed, the variable  $x$  first decreases rapidly to zero (first fast epoch). Then during the increase of the mouth pressure,  $x$  follows zero (first slow epoch) and increases rapidly at  $\tau \approx 0.65$  (second fast epoch). A slow evolution follows corresponding to oscillations of the mouthpiece pressure  $p$  (second slow epoch). Finally,  $x$  decreases again rapidly to zero at  $\tau \approx 1.45$  (third fast epoch) and follows zero slowly (third slow epoch).

In the GSPT framework, the so-called *slow subsystem* is obtained by stating  $\epsilon = 0$  in Eq. (4), which leads to

$$0 = f(x, y) \quad (7a)$$

$$y' = g(y). \quad (7b)$$

The dynamics of (7) approximates the dynamics of (3) (or (4)) during slow epochs. It is restricted to the *critical manifold*  $\mathcal{M}_0$  defined below.

**Definition 4.1.** The critical manifold is defined as

$$\mathcal{M}_0 = \{(x, y) \in \mathbb{R}^2 \mid x = x^*(y)\} \quad (8)$$

with  $x^*(y)$  the branches of the solution of

$$f(x^*(y), y) = 0 \quad (9)$$

in each interval of  $y$  where  $\partial_x f(x, y)$  does not vanish and therefore where we can write that  $f(x, y) = 0$  is equivalent to  $x = x^*(y)$  by the *implicit function theorem*.

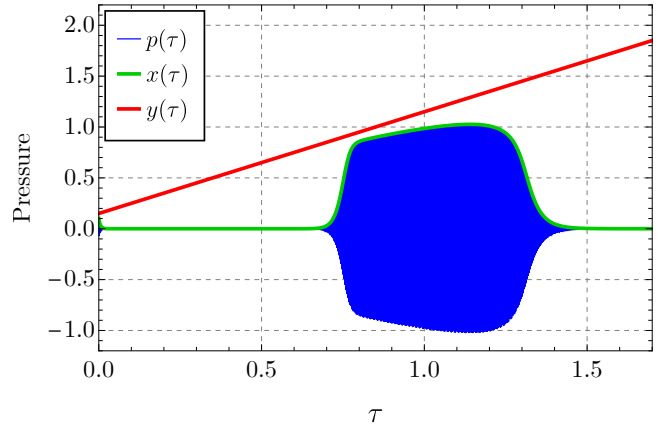


**Figure 2.** Times series  $x(\tau)$  (green) and  $p(\tau)$  (blue) obtained from the numerical integration of the averaged system (4) and of the original system (27) (replacing  $\gamma$  by  $y(t')$  and switching from  $t'$  to  $t$ , see Appendix A), respectively. Both are obtained with  $g(y) = 1$ . The time profile of the linearly increased blowing pressure  $y(\tau)$  is also represented (red). The parameters given in Table 1 are used with  $\epsilon = 0.0183$ . The initial conditions are:  $x(0) = p(0) = 0.1$ ,  $\dot{p}(0) = 0$  and  $y(0) = 0.15$ .

Note that the critical manifold does not depend on the function  $g(y)$ .

Points on the critical manifold are equilibria (or fixed points) of the so-called *fast subsystem* defined by

$$\dot{x} = f(x, y) \quad (10a)$$

$$\dot{y} = 0 \quad (10b)$$

which describes the dynamics of the variable  $x$  for a constant bifurcation parameter. This corresponds to the static case considered in Section 3.

**Definition 4.2.** Let  $a^*(y)$  be the linearization of the fast vector field (10) on  $\mathcal{M}_0$ , i.e., at  $x = x^*(y)$ , defined as

$$a^*(y) = \partial_x f(x^*(y), y) \quad (11)$$

A value  $x^*(y)$  of the fast variable  $x$  is a hyperbolic equilibrium point of (10) if  $a^*(y) \neq 0$ ; stable if  $a^*(y) < 0$  and unstable if  $a^*(y) > 0$ . Then, the critical manifold is called *attracting* (resp. *repelling*) if  $a^*(y) < 0$  (resp.  $a^*(y) > 0$ ) for  $y \in I$  with  $I$  a subset of  $\mathbb{R}$ . A subset  $\mathcal{M}_0^{\text{nh}}$  of the critical manifold  $\mathcal{M}_0$  is *normally hyperbolic* if for each point  $P = (x^*(y), y) \in \mathcal{M}_0^{\text{nh}}$  we have  $a^*(y) \neq 0$ , i.e.,  $\mathcal{M}_0^{\text{nh}}$  is either attracting or repelling<sup>1</sup>.

<sup>1</sup>Normally means that each point of  $\mathcal{M}_0$  must be hyperbolic only in the the direction normal (i.e., non tangent) to itself (see e.g. Definition 2.3.4 and the text below of Ref. [29]).

A simple form of the Fenichel's theorem (from [13]) is given below. It states that all orbits starting near an attracting branch of the critical manifold actually converge to an invariant manifold.

**Theorem 4.1** (Fenichel 1979). *If the critical manifold  $\mathcal{M}_0$  is normally hyperbolic (i.e. attracting or repelling), then there exists a manifold  $\mathcal{M}_\epsilon$ , which is  $\mathcal{O}(\epsilon)$ -close<sup>2</sup> to  $\mathcal{M}_0$  and invariant under the flow (3)<sup>3</sup> (or (4)). The manifold  $\mathcal{M}_\epsilon$  is normally hyperbolic, i.e., it attracts or repels neighboring orbits exponentially fast in directions normal to itself.*

For a more complete statement of the Fenichel's theorem see e.g. Chap. 3 of Ref. [29].

**Definition 4.3.** The manifold  $\mathcal{M}_\epsilon$ , as obtained by the Theorem 4.1, is called the *slow manifold*.

Here and as often, we say “the” manifold  $\mathcal{M}_\epsilon$ . Formally, this is incorrect. Indeed, the complete statement of the Fenichel's theorem stipulates that  $\mathcal{M}_\epsilon$  is usually not unique. However, it also stipulates that all these manifolds are exponentially close to each other, i.e., they lie at a distance [?]  $\mathcal{O}(e^{-K/\epsilon})$  from each other for some  $K > 0$  with  $K = \mathcal{O}(1)$ . Consequently, we adopt the convention to refer to  $\mathcal{M}_\epsilon$  as “the” slow manifold of Eq. (4).

Based on these elements of GSPT, the definition of what we referred to as a *dynamic basin of attraction* is formalized in Section 5.

## 5 Separatrix between dynamic basins of attraction

This section presents the main results of this work. We give in Section 5.1 definitions for general (1,1)-fast-slow systems. The results are then illustrated in Section 5.2.

### 5.1 Definitions and method for computing separatrix between DBAs

The definitions stated in this section are valuable for (1,1)-fast-slow systems in the form of Eq. (3) whose critical manifold  $\mathcal{M}_0$  (see Definition 4.1) has a bistability domain. The definition of the latter is given below.

**Definition 5.1** (Bistability domain of  $\mathcal{M}_0$ ). An open subset

$$D = ]y_l, y_u[ \quad (12)$$

<sup>2</sup>To be understood in the sense of the Hausdorff distance (see e.g. Chap. 3 of Ref. [29]).

<sup>3</sup> $\mathcal{M}_\epsilon$  is called invariant (locally in  $I$ ) under the flow, if  $(x_0, y_0) \in \mathcal{M}_\epsilon$  implies that  $(x(t), y(t)) \in \mathcal{M}_\epsilon$  as long as  $y(t) \in I$  holds.

of  $\mathbb{R}$  is called a *bistability domain* of the critical manifold if for  $y \in D$  Eq. (9) has two attracting branches  $x_1^*(y)$  and  $x_2^*(y)$ , i.e.,  $a_1^*(y) = \partial_x f(x_1^*(y), y) < 0$  and  $a_2^*(y) = \partial_x f(x_2^*(y), y) < 0$ . Necessarily, Eq. (9) has also a repelling branch  $x_3^*(y)$  for which  $a_3^*(y) = \partial_x f(x_3^*(y), y) > 0$ . The critical manifold is non normally hyperbolic at  $y = y_l$  and  $y = y_u$ .

The bistability domain of the critical manifold  $\mathcal{M}_0$  is of course, in the case of a (1,1)-fast-slow system, identical to the bistability domain of the corresponding static problem (see Fig. 1), one has therefore  $y_l = 1.11$  and  $y_u = 1.34$ .

We can now define what we call a *dynamic basin of attraction*.

**Definition 5.2** (Dynamic basin of attraction). In the bistability domain  $D$  (see Definition 5.1) the critical manifold  $\mathcal{M}_0$  of (4) has two coexisting attracting branches  $\mathcal{M}_{0,a_1}$  and  $\mathcal{M}_{0,a_2}$  defined as

$$\mathcal{M}_{0,a_i} = \{x \in \mathbb{R}, y \in D \mid x = x_i^*(y)\}, \quad i = 1, 2 \quad (13)$$

separated by a repelling branch  $\mathcal{M}_{0,r}$

$$\mathcal{M}_{0,r} = \{x \in \mathbb{R}, y \in D \mid x = x_3^*(y)\} \quad (14)$$

Through Fenichel's Theorem 4.1, Eq. (4) has two attracting invariant manifolds  $\mathcal{M}_{\epsilon,a_i}$   $\mathcal{O}(\epsilon)$ -close of  $\mathcal{M}_{0,a_i}$  ( $i = 1, 2$ ) and a repelling slow invariant manifold  $\mathcal{M}_{\epsilon,r}$   $\mathcal{O}(\epsilon)$ -close of  $\mathcal{M}_{0,r}$ . Then the *dynamic basin of attraction* (DBA) of a given attracting branch  $\mathcal{M}_{\epsilon,a_i}$  ( $i = 1, 2$ ) is the subset of the phase space for which orbits originating from initial conditions in the DBA end up following  $\mathcal{M}_{\epsilon,a_i}$  ( $i = 1, 2$ ) when the bistability domain  $D$  is crossed.

We state in Definition 5.2 “end up following” because some transient regimes can exist before the branches  $\mathcal{M}_{\epsilon,a_i}$  ( $i = 1, 2$ ) are reached.

The separatrix between two DBAs and its nature are finally defined.

**Definition 5.3** (Separatrix between DBAs). The *separatrix between DBAs* (SDBA) is the boundary in the phase space that separates two DBAs.

**Definition 5.4** (Nature of the SDBA). The SDBA is the repelling invariant manifold  $\mathcal{M}_{\epsilon,r}$  considered beyond the lower bound  $y_l$  of the bistability domain until a point of the phase space having the smallest physically relevant value of the slow variable  $y$ .

The previous definitions are especially relevant when the increasing blowing pressure does not saturate in the

bistability domain. In such a case, the system has no fixed points (at least it has none for  $y < y_u$ ) and we want to know when the bistability zone is crossed whether or not the original (i.e., non averaged) system oscillates significantly. In the case of musical instrument, this corresponds to the fact that a sound is produced (or not) during the transient. The case of a blowing pressure that saturates in the bistability domain is discussed in Section 6.1.

In view of the definitions 5.3 and 5.4, we are interested in computing the repelling invariant manifold  $\mathcal{M}_{\epsilon,r}$ . Through the Fenichel's theorem 4.1, if  $x^*(y)$  is a normally hyperbolic branch of the critical manifold (either attracting or repelling), the invariant manifold  $\mathcal{M}_\epsilon$  (either attracting or repelling) admits a parametric equation of the form  $x = \bar{x}(y, \epsilon)$ , where  $\bar{x}(y, \epsilon) = x^*(y) + \mathcal{O}(\epsilon)$ . The function  $\bar{x}(y, \epsilon)$  is the solution of  $\epsilon \frac{dx}{dy} = \frac{f(x,y)}{g(x,y)}$  obtained by dividing (4a) by (4b). Asymptotic analytical expressions of  $\bar{x}(y, \epsilon)$ , in the form of a power series in  $\epsilon$ , can be easily obtained in regions in which the critical manifold is hyperbolic (see e.g. Ref. [13]). These approximations fail at non hyperbolic points, making them unusable for our study<sup>4</sup>. Indeed, an SDBA is the extension of a repelling invariant manifold  $\mathcal{M}_{\epsilon,r}$  through non hyperbolic points of the critical manifold (see Definition 5.3). The curve  $\bar{x}(y, \epsilon)$  can be defined as a particular solution of Eq. (3) or Eq. (4). In the manner of Berglund and Landon [15], this particular solution, i.e., the SDBA, is here approximated numerically by means of a time reversal procedure, i.e., by a numerical integration of

$$\epsilon x' = -f(x, y) \quad (15a)$$

$$y' = -g(x, y) \quad (15b)$$

choosing an initial condition  $(x_0, y_0)$  on the upper boundary of the bistability domain  $D$  and on the repelling part  $\mathcal{M}_{0,r}$  of the critical manifold, i.e.,

$$(x_0, y_0) = (x_3^*(y_u), y_u). \quad (16)$$

We use the fact that, through Theorem 4.1,  $\mathcal{M}_{0,r}$  is  $\mathcal{O}(\epsilon)$ -close to the corresponding repelling invariant manifold  $\mathcal{M}_{\epsilon,r}$  which is attracting for (15). The numerical integration is then stopped at the required value of the slow variable  $y$ .

<sup>4</sup>The behavior of a  $(1, 1)$ -fast-slow system near a non hyperbolic point of the critical manifold can be analytically studied by means of the methodology developed by Berglund *et al.* [14, 12] which consists in determining the *scaling law* of the system, i.e., the dependence of the system in the parameter  $\epsilon$  in the neighborhood of the non hyperbolic point. This is not the purpose of the present paper because this analytical method cannot be extended for higher dimensional phase spaces.

The time reversal method has also the advantage to be easily extended to higher dimensional systems (see Section 6.2).

## 5.2 Illustration of SDBAs in the averaged clarinet model with slowly time varying blowing pressure

The attracting and repelling branches of the critical manifold  $\mathcal{M}_0$  of Eq. (4) with the parameters given in Table 1 are respectively the stable and unstable branches of the bifurcation diagram depicted in Fig. 1 (see Definition 4.1 and the beginning of Section 3). The bistability domain of  $\mathcal{M}_0$ , as described by Definition 5.1, is  $D = [y_l = 1.11, y_u = 1.34]$ . In the latter, the DBAs of each attracting invariant manifold  $\mathcal{M}_{\epsilon,a_1}$  and  $\mathcal{M}_{\epsilon,a_2}$  (see Definition 5.2) are denoted DBA<sub>1</sub> and DBA<sub>2</sub>, respectively. Without loss of generality, we chose arbitrarily that  $\mathcal{M}_{\epsilon,a_1}$  is the branch corresponding to  $x_1^*(y) = 0$ . The separatrix between DBA<sub>1</sub> and DBA<sub>2</sub> is obtained through Definition 5.4. It is the extended slow repelling invariant manifold  $\mathcal{M}_{\epsilon,r}$  (associated to the repelling branch  $\mathcal{M}_{0,r}$  of the critical manifold) beyond the lower bound  $y_l$  of the bistability domain to a point of the phase space having the smallest possible value of the slow variable  $y$ . In system (15) with a linear time variation of  $y$ , i.e.,  $g(y) = 1$ ,  $x(\tau)$  diverges as  $\tau$  tends to infinity. Consequently, the SDBA is approximated by an orbit of Eq. (15) having the appropriate initial condition given by (16). Here that yields  $(x_0, y_0) = (x_3^*(y_u) = 0.95, y_u = 1.34)$ . As mentioned in Section 5.1, this orbit is obtained by a numerical simulation. The simulation is stopped when an arbitrary large value of  $x(\tau)$  is reached. The resulting times series are shown in Fig. 3(a) (red solid and dashed lines for  $x(\tau)$  and  $y(\tau)$ , respectively).

Fig. 3(b) shows the time integration of the direct time system (4) with an initial condition (IC) first in DBA<sub>1</sub> (in blue) and then in DBA<sub>2</sub> (in green). Both of these initial conditions are chosen close to the SDBA. In the case of IC  $\in$  DBA<sub>1</sub>, we observe that  $x(\tau)$  first rapidly approaches zero and remains equal to zero over time. In the case of IC  $\in$  DBA<sub>2</sub>, similarly to the example in Fig. 2, after a first similar start transient,  $x(\tau)$  remains close to zero for a moment and then moves away from it, taking a non-zero value for a period of time before falling back to zero. The first (resp. second) situation seems to correspond well to the case where the trajectory tends to follow  $\mathcal{M}_{\epsilon,a_1}$  (resp.  $\mathcal{M}_{\epsilon,a_2}$ ) when the bistability domain  $D$  is crossed. This appears more clearly in Fig. 3(c) in which the orbits previously computed are represented in the phase plane and superimposed to the critical manifold. The stream plot of the vector field Eq. (4) is also shown. The latter shows, for  $y < y_u$ , that the orbits starting with an initial

condition in the DBA<sub>1</sub> (resp. DBA<sub>2</sub>), i.e., below (resp. above) the SDBA, end up following  $\mathcal{M}_{\epsilon, a_1}$  (resp.  $\mathcal{M}_{\epsilon, a_2}$ ).

To better understand what happens in the vicinity of the  $y$ -axis, a logarithmic scale is used in Fig. 3(d) for the ordinates. This example shows that very small amplitudes are encountered. In a real-world problems, residual noise would prevent reaching such low amplitudes. In the future, stochastic studies (similar to what was done in Ref. [10]) would be relevant to complete this work.

The transient regimes mentioned after Definition 5.2 are visible in the stream plot in Fig. 3(c). These transient regimes are all the longer as the initial conditions are chosen close to the SDBA. This begs the following question: will these transients be short enough for the system to reach the branches  $\mathcal{M}_{\epsilon, a_i}$  before the end of the bistability domain? This question relates to the link between the duration of transients and the distance between the initial conditions and the SDBA. This will be explored in future works.

Examples similar to those of Figs. 3(c) and 3(d) are shown in Fig. 4 for two other values of the parameter  $\epsilon$ :  $\epsilon = 0.00366 < 0.0183$  (see Fig. 4(a)) and  $\epsilon = 0.0732 > 0.0183$  (see Fig. 4(b)). This shows that the smaller  $\epsilon$ , the shorter (in terms of  $y$ ) the above-mentioned transients, and the more visible the distinction between slow and fast phases. In Fig. 4(b) in particular (top, blue line) the orbit is still relatively far from the  $\mathcal{M}_{\epsilon, a_2}$  (the  $y$ -axis) when the upper bound of the bistability domain is reached. This highlights the limits of the approach for large values of  $\epsilon$ . Nevertheless, the approach allows to interpret these borderline situations.

## 6 Discussion

### 6.1 Case of a blowing pressure saturating in the bistability domain

In this section the case where the blowing pressure tends towards a finite limit  $y_{\text{targ}}$  in the bistability domain is explored. More precisely, an exponential growth of the blowing pressure is considered using  $g(y) = y_{\text{targ}} - y$  (with  $y_{\text{targ}} \in D$ ) which yields

$$y(\tau) = y_{\text{targ}} + (y_0 - y_{\text{targ}})e^{-\tau}, \quad (17)$$

with again  $y_0 = y(0)$ . Written in the slow timescale  $\tau$ , the system takes the following form

$$\epsilon x' = f(x, y) \quad (18a)$$

$$y' = y_{\text{targ}} - y. \quad (18b)$$

This differs from the case studied so far, in which the pressure does not saturate. Here fixed points are solutions

of  $f(x, y) = 0$  and  $y_{\text{targ}} - y = 0$ , that leads to  $f(x, y_{\text{targ}}) = 0$  and  $x = x_i^*(y_{\text{targ}})$  ( $i = 1, 2, 3$ ). Therefore, the points  $P_i^* = (x_i^*(y_{\text{targ}}), y_{\text{targ}})$  ( $i = 1, 2, 3$ ) are the fixed points of Eq. (18). The Jacobian matrices  $\mathbf{J}(P_i^*)$  of (18) evaluated at each fixed point  $P_i^*$  are

$$\mathbf{J}(P_i^*) = \begin{pmatrix} a_i^*(y_{\text{targ}}) & \frac{\partial_y f(x_i^*(y_{\text{targ}}), y_{\text{targ}})}{\epsilon} \\ \epsilon & -1 \end{pmatrix} \quad (19)$$

whose eigenvalues are  $\mu_1 = \frac{a_i^*(y_{\text{targ}})}{\epsilon}$  and  $\mu_2 = -1$ . Because  $a_1^*(y_{\text{targ}}) < 0$ ,  $a_2^*(y_{\text{targ}}) < 0$  and  $a_3^*(y_{\text{targ}}) > 0$  (see Definition 5.1),  $P_1^*$  and  $P_2^*$  are *nodes* (i.e.,  $\mu_1 \mu_2 > 0$ ) and  $P_3^*$  is a *saddle* (i.e.,  $\mu_1 \mu_2 < 0$ ). These classical definitions of nodes and saddle are taken from Ref. [32].

The problem therefore becomes a classic problem of finding the basins attraction of stable fixed points of a 2-dimensional system. In this case, the DBAs of the attracting branches  $\mathcal{M}_{\epsilon, a_i}$  ( $i = 1, 2$ ) and the SBAs of the fixed points  $P_1^*$  and  $P_2^*$  are identical. The separatrix between these basins is the stable manifold of the unstable fixed point  $P_3^*$  [17]. The latter is again computed using a time reversal simulation. The following equation

$$\epsilon x' = -f(x, y) \quad (20a)$$

$$y' = -y_{\text{targ}} + y. \quad (20b)$$

is numerically integrated from initial condition chosen as a small perturbation of  $P_3^*$ .

An example is shown in Fig. 5. Figures 5(a) and 5(b) show similar representations as in Figs 3(c) and 3(d), respectively. In Fig. 5(a) the orange vertical line indicates the target value  $y_{\text{targ}}$  of the mouth pressure. Intersections between this vertical line and the critical manifold correspond to fixed points of (18). Importantly, the critical manifold is independent of the function  $g(y)$  and therefore identical to the one previously obtained in Section 5.2 for a linear growth of  $y$ . Still in Fig. 5(a), a zoom near the unstable fixed point  $P_3^*$  is performed to highlight its stable manifold interpreted here as a SDBA (represented by a red line in the figure). We can see in Fig. 5(b) that the SDBA intersects the  $x$ -axis for a value of  $y$  just below 0.01.

Two orbits obtained by numerical integration of the direct time system Eq. (18) with (i) a IC first in DBA<sub>1</sub> (in blue) and (ii) in DBA<sub>2</sub> (in green) also appear in Fig. 5. The corresponding time series are plotted in Figs. 5(d) and 5(c), respectively. In the case of IC  $\in$  DBA<sub>1</sub>, the orbit stays close to the  $y$ -axis for a moment and then moves away from it, follows the branch  $\mathcal{M}_{\epsilon, a_1}$  of the critical manifold before stopping at  $P_1^*$ . For IC  $\in$  DBA<sub>2</sub>, it is the point  $P_2^*$  which ends up being reached. Here too transients are observed before the fixed points are reached.

## 6.2 DBA and SDBA to more realistic models

This work introduces the notions of DBA and SDBA for (1,1)-fast-slow systems. However, more realistic models of reed instruments cannot be reduced to (1,1)-fast-slow systems. Working in the plane makes it easier to illustrate and understand these concepts. However, the concepts of DBA and SDBA can be generalized to  $(m,n)$ -fast-slow systems. Indeed, the SDBA is a particular solution of the considered system. However, there are two things to bear in mind when the fast subsystem is more than one-dimensional. Firstly, the critical manifold is also more than one-dimensional and it can be attracting (if all eigenvalues of the Jacobian matrix of the fast subsystem evaluated on the critical manifold have negative real parts), repelling (if all the eigenvalues have positive real parts) and *saddle-type* (if there are eigenvalues with negative real parts and others with positive real parts). Previous definitions are taken from Ref. [29] (Chap. 3). In this case of a saddle-type invariant manifold, the SDBA cannot be obtained by reversing the time, as presented above for a purely repelling manifold. Indeed, a saddle-type manifold in direct time remains saddle-type in reverse time. In this case methods of continuation of orbits could be used, for example using the software AUTO [20]. The second thing to consider is that the fast subsystem can have other types of than equilibria; such as periodic or quasiperiodic solutions. The complete bifurcation diagram of the fast subsystem (including periodic solutions and if possible quasiperiodic solutions) is not anymore the critical manifold of the studied  $(m,n)$ -fast-slow system which includes only the equilibrium solutions. In a  $(m,n)$ -fast-slow system, invariant manifolds associated to quasiperiodic solutions of the fast subsystem are more complicated to deal with, both analytically and computationally. However, periodic solutions can be treated in the same way as equilibrium solutions. First, because theoretically Berglund [12] proposes an analogue of Fenichel's theorem on the existence of an invariant manifold tracking families of periodic orbits and also because periodic solutions are easy to compute numerically. As in the case of equilibrium solutions, for the time reversal method to be used, the invariant manifold considered for the SDBA calculation must be repelling. For periodic solutions, that means that  $m - 1$ <sup>5</sup> of the *Floquet multipliers* associated with the periodic solution under consideration have modulus strictly larger than one (see e.g. Ref. [32], Chap. 7, for details about local stability of periodic solutions).

We provide here an illustration for the original system

<sup>5</sup>A periodic solution of an  $m$ -dimensional fast subsystem is associated to  $m$  Floquet multipliers but one is always unity (see Lemma 7.3 of Ref. [32]).

(27) (replacing  $\gamma$  par  $y(t')$  and switching from  $t'$  to  $t$ , see Appendix A), a (2,1)-fast-slow system (globally 3-dimensional) since the 1-dimensional complex Eq. (33) is a 2-dimensional real equation.

As mentioned above, the trivial fixed point of the fast subsystem (10) associated to the averaged dynamics (3) is the equilibrium solution of the original non-averaged dynamics (27) and non trivial fixed points correspond to periodic solutions of (27). In the bistability domain the fast subsystem associated to the original dynamics has thus a stable equilibrium solution, a stable and an unstable periodic solutions. The manifolds corresponding to these periodic solutions are represented in Fig. 6 by gray and black surfaces in the  $(y, p, \dot{p})$ -space, respectively. In practice these manifolds, which also represent the static bifurcation diagram of the original dynamical system, are deduced from the critical manifold of Eq. (3). Indeed, in the  $(p, \dot{p})$ -plane periodic solutions of the non-averaged dynamics (27) is a circle whose radius is equal to the value of the corresponding fixed point of Eq. (3). The manifolds of the periodic solutions of the latter are then obtained by rotation of the critical manifold of Eq. (3) around the  $y$ -axis.

The SDBA is here the extension of a 2-dimensional repelling slow invariant manifold associated to the unstable periodic solution of the fast subsystem. In a 2-dimensional system an unstable periodic solution is associated to two Floquet multipliers, one is unity [?] and the other has modulus larger than one. Therefore, the associated invariant manifold is repelling and the reverse time procedure can be used.

In Fig. 6 the SDBA is shown in red in the  $(y, p, \dot{p})$ -space. Although the SDBA is 2-dimensional, here we computed only one solution of the time-reversed system for initial conditions on the periodic solution at  $y = y_u$ . Here, the period of oscillations is short enough for the two-dimensional SDBA to be represented correctly by a single periodic orbit.

Results of time-domain simulation of the (2,1)-fast-slow original system (in direct time) with two different sets of initial conditions, one in  $DBA_1$  (in blue) and the second one in  $DBA_2$  (in green) are also shown in Fig. 6. The parameters and IC are the same as the same as in Fig. 3 (same parameters and initial conditions) and similar observations can be made: when  $IC \in DBA_1$ , the orbit first winds around the  $y$ -axis and remains in the vicinity of it. Conversely, when  $IC \in DBA_2$ , after a first similar start transient, the orbits stays on vicinity of the  $y$ -axis for a while and then moves away to reach the manifold associated to the stable periodic solution. The simulation is carried out over a shorter period of time than in Fig. 3. This is why we do not observe the orbit falling back to

zero.

## 7 Conclusion

In this paper the behavior of a class of one-dimensional non-autonomous dynamical systems has been investigated. These systems are obtained by slowly varying over time the bifurcation parameter of the corresponding autonomous systems (called fast subsystem in the paper) whose bifurcation parameter is constant. More precisely, the case considered corresponds to the time-varying parameter crossing a bistability domain of the associated autonomous system. The proposed methodology has been illustrated on a simple musical reed instrument model.

In the bistability domain, the non-autonomous system has attracting manifolds (resp. a repelling manifold) associated with the two stable branches (resp. unstable branch) of the bifurcation diagram of the corresponding autonomous system. The concept of dynamic basin of attraction (DBA) of a given attracting manifold has been introduced and defined as the set of initial conditions in the phase space (in which the time-varying parameter is considered as another state variable) from which the orbits end up following this attracting manifold. The separatrix between two DBAs (SDBA), i.e., the boundary in the phase space that separates the two DBAs, has been defined as the repelling invariant manifold mentioned above and considered beyond the lower bound of the bistability domain until a point of the phase space having the smallest possible value of the time-varying bifurcation parameter. In practice, the separatrix has been computed using a numerical reverse time integration with relevant initial conditions.

As a first perceptive, keep working on low dimension systems, it would be interesting to develop analytical methods that would make it possible to relate the characteristics of the time-varying parameter to the nature of the observed regime. Moreover, in the purpose of real-life applications, the method should be extended to more complex dynamic systems. First, the notions of DBA and SDBA remain valid for high dimensional systems. However, if the solutions (stable and unstable) of the multistable autonomous system are more complex than equilibria, the challenge will be to detect the unstable solutions to then deduce the possible SDBAs of the non-autonomous system. Secondly, multistable systems are known to be very sensitive to noise. Therefore, the influence of noise on SDBAs should be studied in the future.

Finally, we believe that the general nature of the method suggests that the results obtained go beyond musical acoustics. Application in physics, neuroscience or

climate science can be envisaged, in particular to deal with the so-called critical transition problems.

## Data Availability Statement

The data that support the findings of this study are available from the corresponding author upon reasonable request.

## A Derivation of the model

### A.1 Classical single reed instrument model

Sound production by single reed instruments is classically modeled through the nonlinear coupling between two linear components [5, 24, 16]: the reed and the air-column inside the instrument. While blowing air through the reed channel into the instrument, the instrumentalist provides a quasi-static source of energy. The instrument and the player constitute an autonomous dynamical system. When the trivial equilibrium solution of this system becomes unstable, a sound is produced [36, 23, 33].

Since the lowest resonance frequency of the reed is one order of magnitude higher than the sound frequency for many notes, the reed is often modeled as a lossless stiffness spring [4, 30]. Therefore its position relative to rest is proportional to the pressure drop across the reed, i.e., the pressure difference between the mouth and the mouthpiece of the instrument. The linear pressure response of the air column  $P$  to the volume flow  $U$  through the reed channel is given in the frequency domain through the input impedance of the air column  $Z$

$$P(\omega) = Z(\omega)U(\omega), \quad (21)$$

where  $\omega$  is the angular frequency. We point out that the model presented in the appendix already considers a dimensionless pressure and flow (see Chap. 9 of Ref. [16] for more details on the model).

The contribution at the input of the instrument of the (infinite) series of modes of the air column is taken into account in  $Z(\omega)$ . For computational reasons, the series is truncated to  $N$  modes, where  $N$  is an integer:

$$Z(\omega) = \sum_{n=1}^N Z_n \frac{j\epsilon_n \omega_n \omega}{\omega_n^2 + j\epsilon_n \omega_n \omega - \omega^2}, \quad (22)$$

with  $Z_n$ ,  $\omega_n$  and  $\epsilon_n$  the modal parameters, respectively the modal factor, the resonance angular frequency and the inverse of the quality factor of the  $n^{\text{th}}$  peak of the impedance (corresponding to the  $n^{\text{th}}$  mode of the air column). Eq. (22) can be written in the time domain

$$d_{t''t''} p_n + \epsilon_n \omega_n d_{t''} p_n + \omega_n^2 p_n = Z_n \epsilon_n \omega_n d_{t''} u, \quad \forall n \in [1, N], \quad (23)$$

in which  $t''$  is used to denote the original timescale,  $u$  is the inverse Fourier transform of  $U$  and  $p_n$  is such that  $p = \sum_{i=1}^N p_n$ , where  $p$  is the inverse Fourier transform of  $P$  [33] and corresponds to the time evolution of the mouthpiece pressure.

Through Bernoulli's principle, the volume flow through the reed channel  $u$  is related nonlinearly to the reed channel opening and the pressure difference between the mouth and the mouthpiece [26, 19]

$$u = \hat{F}(p, \gamma) = \zeta(1+p-\gamma)\sqrt{|\gamma-p|} \operatorname{sgn}(\gamma-p)H(1+p-\gamma) \quad (24)$$

where  $H$  is the Heaviside function,  $\gamma$  is the dimensionless pressure in the mouth of the musician and  $\zeta$  a dimensionless parameter accounting for many embouchure parameters. The parameters  $\gamma$  and  $\zeta$  are the *control (or bifurcation) parameters* of the model. The relation (24) is called the nonlinear characteristic (NLC) of the instrument exciter. In this work a polynomial fitting of the function  $\hat{F}(p, \gamma)$  (see Eq. (24)), denoted  $F(p, \gamma)$ , is obtained using the function `InterpolatingPolynomial` of the Mathematica software [37] (see Fig. 7).

Using the function  $F(p, \gamma)$ , Eq. (23) can be written using only the pressure  $p$  as follows

$$d_{t'} p_n + \epsilon_n \omega_n d_{t'} p_n + \omega_n^2 p_n - Z_n \epsilon_n \omega_n d_{t'} p_n \partial_p F(p, \gamma) = 0, \quad \forall n \in [1, N]. \quad (25)$$

A minimal model of a reed instrument including a single mode of the air-column is obtained by stating  $N = 1$ . In this case (25) becomes

$$d_{t'} p + \epsilon_1 \omega_1 d_{t'} p + \omega_1^2 p - Z_1 \epsilon_1 \omega_1 d_{t'} p \partial_p F(p, \gamma) = 0 \quad (26)$$

In this case ( $N = 1$ ), since  $p_1 = p$ ,  $p_1$  is replaced by  $p$  in Eq. (26). This is clearly a minimal yet useful model of sound production in reed instruments. Indeed, it takes into account the two main control parameters,  $\gamma$  et  $\zeta$ , adjusted by the musician and describes the physical mechanism through which sound emerges from the trivial equilibrium (i.e. silence) when a resonance of the air column is excited by an incoming flow. We finally introduce the dimensionless time  $t' = \omega_1 t''$ , so Eq. (26) takes the form of the following self-excited oscillator

$$d_{t'} p + \epsilon_1 h(p, d_{t'} p, \gamma) + p = 0. \quad (27)$$

where

$$h(p, d_{t'} p, \gamma) = d_{t'} p (1 - Z_1 \partial_p F(p, \gamma)). \quad (28)$$

## A.2 Averaged dynamics with a slowly time-varying control parameter

Eq. (27), in the phase space  $(p, d_{t'} p)$ , is transformed to a slowly varying system using the following complex repre-

sentation introducing a new variable  $\xi$  as

$$\xi e^{jt'} = d_{t'} p + jp \quad (29)$$

with  $j^2 = -1$ . Combining Eq. (29) and its complex conjugate yields the expressions of  $p$  and  $d_{t'} p$  as functions of  $\xi$

$$p = \frac{\xi e^{jt'} - \xi^* e^{-jt'}}{2j}, \quad (30)$$

$$d_{t'} p = \frac{\xi e^{jt'} + \xi^* e^{-jt'}}{2}, \quad (31)$$

where  $\xi^*$  is the complex conjugate of  $\xi$ . Deriving Eq. (29) with respect to  $t'$  and using Eq. (31) give  $d_{t'} p$  as

$$d_{t'} p = d_{t'} \xi e^{jt'} + j \xi e^{jt'} - \frac{j}{2} (\xi e^{jt'} + \xi^* e^{-jt'}). \quad (32)$$

Substituting Eqs. (30), (31) and (32) into Eq. (27) yields the following complex non-autonomous system

$$d_{t'} \xi = -\epsilon_1 h \left( \frac{\xi e^{jt'} - \xi^* e^{-jt'}}{2j}, \frac{\xi e^{jt'} + \xi^* e^{-jt'}}{2}, \gamma \right) e^{-jt'}. \quad (33)$$

Then, stating  $\xi = x e^{j\phi}$  and  $\phi = t' + \varphi$  and separating real and imaginary parts of each side of Eq. (33) gives

$$d_{t'} x = -\epsilon_1 h(x \sin \phi, x \cos \phi, \gamma) \cos \phi, \quad (34a)$$

$$d_{t'} \phi = 1 + \epsilon_1 h(x \sin \phi, x \cos \phi, \gamma) \frac{\sin \phi}{x}. \quad (34b)$$

Since  $0 < \epsilon_1 \ll 1$ , Eq. (34) is simplified by means of an averaging method (see Chap. 7 of Ref. [31]) to

$$d_{t'} x = \epsilon_1 f(x, \gamma), \quad (35a)$$

$$d_{t'} \phi = 1 \quad (35b)$$

where  $x$  and  $\phi$  are uncoupled and

$$f(x, \gamma) = -\frac{1}{2\pi} \int_0^{2\pi} h(x \sin \alpha, x \cos \alpha, \gamma) \cos \alpha d\alpha. \quad (36)$$

Details on the averaging procedure are provided in Section B.

The integral in Eq. (36) is generally hard to solve analytically, except if the function  $h$  is assumed to have a polynomial form. This is the case here using the polynomial fitting  $F(p, \gamma)$  of the NLC.

The dynamics of the mouth pressure (now denoted  $y$ ) is finally added as  $d_{t'} y = \hat{\epsilon} g(y)$ . Then, assuming  $\hat{\epsilon}/\epsilon_1 \ll 1$ , switching the time from  $t'$  to  $t = \epsilon_1 t'$  and using the notation  $\{\} = d_t \{\}$ , the following system is obtained

$$\dot{x} = f(x, y) \quad (37a)$$

$$\dot{y} = \epsilon g(y) \quad (37b)$$

where  $\epsilon$  is defined as

$$\epsilon = \frac{\hat{\epsilon}}{\epsilon_1} \quad (38)$$

which is the relevant small parameter to use for this model.

## B Details on the averaging procedure

Omitting here, for the sake of clarity, the dependence in  $\gamma$ , and introducing

$$X(x, \phi) = -h(x \sin \phi, x \cos \phi, \gamma) \cos \phi, \quad (39a)$$

$$\Omega(x, \phi) = h(x \sin \phi, x \cos \phi, \gamma) \frac{\sin \phi}{x}, \quad (39b)$$

Eq. (34) becomes

$$d_{t'}x = \epsilon_1 X(x, \phi), \quad (40a)$$

$$d_{t'}\phi = 1 + \epsilon_1 \Omega(x, \phi). \quad (40b)$$

The latter is a (1,1)-fast-slow systems with  $t'$  the fast timescale,  $x$  the slow variable and  $\phi$  the fast variable. The principle of the average procedure (see Chap. 7 of Ref. [31]), consists in assuming the following form for the variable  $x$

$$x = v + \epsilon_1 u(v, \phi) \quad (41)$$

with  $u(v, \phi)$  a function  $2\pi$ -periodic in  $\phi$ .

Using Eq. (41) and

$$d_{t'}u = (1 + \epsilon_1 \Omega(v + \epsilon_1 u, \phi)) \partial_\phi u + d_{t'}v \partial_v u, \quad (42)$$

Eq. (40a) becomes

$$d_{t'}v(1 + \epsilon_1 \partial_v u) + \epsilon_1 (1 + \epsilon_1 \Omega(v + \epsilon_1 u, \phi)) \partial_\phi u = \epsilon_1 X(v + \epsilon_1 u, \phi). \quad (43)$$

Each  $\epsilon_1$ -dependent function in (43) is expanded in a first-order Taylor series around  $\epsilon_1 = 0$ , that yields

$$d_{t'}v + \epsilon_1 (1 + \epsilon_1 \Omega(v, \phi) + \mathcal{O}(\epsilon_1^2)) (1 - \epsilon_1 \partial_v u + \mathcal{O}(\epsilon_1^2)) \partial_\phi u = (\epsilon_1 X(v, \phi) + \mathcal{O}(\epsilon_1^2)) (1 - \epsilon_1 \partial_v u + \mathcal{O}(\epsilon_1^2)) \quad (44)$$

which simplifies into

$$d_{t'}v = \epsilon_1 (X(v, \phi) - \partial_\phi u) + \mathcal{O}(\epsilon_1^2) \quad (45)$$

Then one assumes a function  $u(v, \phi)$  which satisfies the following equation

$$\partial_\phi u = X(v, \phi) - f(v). \quad (46)$$

Integrating (46) with respect to  $\phi$  from 0 to  $2\pi$  and because  $u(v, \phi)$  is  $2\pi$ -periodic in  $\phi$  we obtain

$$f(v) = \frac{1}{2\pi} \int_0^{2\pi} X(v, \alpha) d\alpha, \quad (47)$$

and then  $f(v)$  is the average of  $X(v, \phi)$  as defined in Eq. (36).

Substituting (46) into (45) and adding Eq. (40b) we obtain a simplified dynamical system with the following form

$$d_{t'}v = \epsilon_1 f(v) + \mathcal{O}(\epsilon_1^2) \quad (48a)$$

$$d_{t'}\phi = 1 + \mathcal{O}(\epsilon_1). \quad (48b)$$

Finally, consistently with  $0 < \epsilon_1 \ll 1$ , we have  $\epsilon_1 f(v) + \mathcal{O}(\epsilon_1^2) \approx \epsilon_1 f(v)$ ,  $1 + \mathcal{O}(\epsilon_1) \approx 1$  and  $v \approx x$  and therefore Eq. (35) is proven.

## References

- [1] Alkhayuon, H.M., Ashwin, P.: Rate-induced tipping from periodic attractors: Partial tipping and connecting orbits. *Chaos: An Interdisciplinary Journal of Nonlinear Science* **28**(3), 033,608 (2018). DOI 10.1063/1.5000418. URL <https://pubs.aip.org/cha/article/28/3/033608/1059619/Rate-induced-tipping-from-periodic-attractors>
- [2] Ashwin, P., Perryman, C., Wiczeorek, S.: Parameter shifts for nonautonomous systems in low dimension: bifurcation- and rate-induced tipping. *Nonlinearity* **30**(6), 2185–2210 (2017). DOI 10.1088/1361-6544/aa675b. URL <https://iopscience.iop.org/article/10.1088/1361-6544/aa675b>
- [3] Ashwin, P., Wiczeorek, S., Vitolo, R., Cox, P.: Tipping points in open systems: bifurcation, noise-induced and rate-dependent examples in the climate system. *Philosophical Transactions of the Royal Society A: Mathematical, Physical and Engineering Sciences* **370**(1962), 1166–1184 (2012). DOI 10.1098/rsta.2011.0306. URL <https://royalsocietypublishing.org/doi/10.1098/rsta.2011.0306>
- [4] Backus, J.: Small-vibration theory of the clarinet. *J. Acoust. Soc. Am.* **35**(3), 305–313 (1963). DOI 10.1121/1.1918458
- [5] Benade, A.H.: *Fundamentals of musical acoustics*. Oxford University Press (1976)
- [6] Benoît, E.: *Dynamic bifurcations*. In: *Lect. Notes Math.*, vol. 1493. Springer (Actes de la condérence tenue à Luminy, Marseilles, France, du 5 au 10 mars 1990)
- [7] Bergeot, B., Almeida, A., Vergez, C., Gazengel, B.: Prediction of the dynamic oscillation threshold in a clarinet model with a linearly increasing blowing pressure. *Nonlinear Dynamics* **73**(1-2), 521–534 (2013). DOI 10.1007/s11071-013-0806-y

- [8] Bergeot, B., Almeida, A., Vergez, C., Gazengel, B.: Prediction of the dynamic oscillation threshold in a clarinet model with a linearly increasing blowing pressure: influence of noise. *Nonlinear Dynamics* **74**(3), 591–605 (2013). DOI 10.1007/s11071-013-0991-8
- [9] Bergeot, B., Almeida, A., Vergez, C., Gazengel, B., Ferrand, D.: Response of an artificially blown clarinet to different blowing pressure profiles. *J. Acoust. Soc. Am.* **135**(1), 479–490 (2014)
- [10] Bergeot, B., Vergez, C.: Analytical prediction of delayed hopf bifurcations in a simplified stochastic model of reed musical instruments. *Nonlinear Dynamics* **107**, 3291–3312 (2022). DOI 10.1007/s11071-021-07104-9
- [11] Berglund, N.: Dynamic Bifurcations: Hysteresis, Scaling Laws and Feedback Control. *Progress of Theoretical Physics Supplement* **139**, 325–336 (2000). DOI 10.1143/PTPS.139.325. URL <https://academic.oup.com/ptps/article-lookup/doi/10.1143/PTPS.139.325>
- [12] Berglund, N., Gentz, B.: Noise-induced phenomena in slow-fast dynamical systems, A sample-paths approach. *Probability and its Applications (New York)*. Springer-Verlag London Ltd. (2006)
- [13] Berglund, N., Gentz, B.: Stochastic dynamic bifurcations and excitability. *Stochastic Methods in Neuroscience* (2010). DOI 10.1093/acprof:oso/9780199235070.003.0003
- [14] Berglund, N., Kunz, H.: Memory effects and scaling laws in slowly driven systems. *J. Phys. A: Math. Gen* **32**, 15–39 (1999). DOI 10.1088/0305-4470/32/1/005. URL <http://iopscience.iop.org/0305-4470/32/1/005>
- [15] Berglund, N., Landon, D.: Mixed-mode oscillations and interspike interval statistics in the stochastic FitzHugh–Nagumo model. *Nonlinearity* **25**(8), 2303–2335 (2012). DOI 10.1088/0951-7715/25/8/2303. URL <https://iopscience.iop.org/article/10.1088/0951-7715/25/8/2303>
- [16] Chaigne, A., Kergomard, J.: *Acoustics of Musical Instruments. Modern Acoustics and Signal Processing*. Springer-Verlag New York (2016). DOI 10.1007/978-1-4939-3679-3
- [17] Chiang, H.D., Hirsch, M., Wu, F.: Stability regions of nonlinear autonomous dynamical systems. *IEEE Transactions on Automatic Control* **33**(1), 16–27 (1988). DOI 10.1109/9.357. URL <http://ieeexplore.ieee.org/document/357/>
- [18] Colinot, T., Vergez, C., Guillemain, P., Doc, J.B.: Multi-stability of saxophone oscillation regimes and its influence on sound production. *Acta Acustica* **5**, 33 (2021). DOI 10.1051/aacus/2021026. URL <https://acta-acustica.edpsciences.org/10.1051/aacus/2021026>
- [19] Dalmont, J.P., Gilbert, J., Ollivier, S.: Nonlinear characteristics of single-reed instruments: Quasistatic volume flow and reed opening measurements. *J. Acoust. Soc. Am.* **114**(4), 2253–2262 (2003). DOI 10.1121/1.1603235
- [20] Doedel, E.J., Oldeman, B.: *Auto-07p: continuation and bifurcation software*. Montreal, QC: Concordia University Canada (1998). URL <http://indy.cs.concordia.ca/auto/>
- [21] Fenichel, N.: Geometric singular perturbation theory for ordinary differential equations. *Journal of Differential Equations* **98**, 53–98 (1979). URL <http://scholar.google.com/scholar?hl=en&btnG=Search&q=intitle:Geometric+Singular+Perturbation+Theory+Ordinary+Differential+Equations#0>
- [22] Feudel, U., Pisarchik, A.N., Showalter, K.: Multistability and tipping: From mathematics and physics to climate and brain—Minireview and preface to the focus issue. *Chaos: An Interdisciplinary Journal of Nonlinear Science* **28**(3), 033,501 (2018). DOI 10.1063/1.5027718. URL <https://pubs.aip.org/cha/article/28/3/033501/1059586/Multistability-and-tipping-From-mathematics-and>
- [23] Fletcher, N.: Nonlinear theory of musical wind instruments. *Applied Acoustics* **30**(2-3), 85 – 115 (1990). DOI 10.1016/0003-682X(90)90040-2
- [24] Fletcher, N.H., Rossing, T.D.: *The physics of musical instruments*. Springer-Verlag (New York, 1991)
- [25] Gilbert, J., Maugeais, S., Vergez, C.: Minimal blowing pressure allowing periodic oscillations in a simplified reed musical instrument model: Bouasse–Benade prescription assessed through numerical continuation. *Acta Acustica* **4**(27), 12 (2020). DOI 10.1051/aacus/2020026
- [26] Hirschberg, A.: Aero-acoustics of wind instruments. In: *Mechanics of musical instruments by A. Hirschberg/ J. Kergomard/ G. Weinreich*, vol. 335 of *CISM Courses and lectures*, chap. 7, pp. 291–361. Springer-Verlag (1995)
- [27] Jones, C.K.: Geometric singular perturbation theory. In: R. Johnson (ed.) *Dynamical Systems, Lecture Notes in Mathematics*, vol. 1609, pp. 44–118. Springer Berlin Heidelberg (1995). DOI 10.1007/BFb0095239
- [28] Kuehn, C.: Multiple Time Scale Dynamics, *Applied Mathematical Sciences*, vol. 191, 1st edn., chap. 12. Springer International Publishing (2015). DOI <https://doi.org/10.1007/978-3-319-12316-5>
- [29] Kuehn, C.: Multiple Time Scale Dynamics, *Applied Mathematical Sciences*, vol. 191, 1st edn. Springer International Publishing (2015). DOI <https://doi.org/10.1007/978-3-319-12316-5>
- [30] Ollivier, S., Dalmont, J.P., Kergomard, J.: Idealized models of reed woodwinds. part 1 : Analogy with bowed string. *Acta. Acust. Acust.* **90**, 1192–1203 (2004)
- [31] Sanders, J.A., Verhulst, F., Murdock, J.A.: *Averaging methods in nonlinear dynamical systems*, 2nd edn. No. v. 59 in *Applied mathematical sciences*. Springer, New York (2007)
- [32] Seydel, R.: *Practical Bifurcation and Stability Analysis, Interdisciplinary Applied Mathematics*, vol. 5, 3ième edn. Springer (2010)

- [33] Silva, F., Kergomard, J., Vergez, C., Gilbert, J.: Interaction of reed and acoustic resonator in clarinet-like systems. *J. Acoust. Soc. Am.* **124**(5), 3284–3295 (2008)
- [34] Tredicce, J.R., Lippi, G.L., Mandel, P., Charasse, B., Chevalier, A., Picqué, B.: Critical slowing down at a bifurcation. *Am. J. Phys.* **72**(6), 799–809 (2004)
- [35] Wieczorek, S., Ashwin, P., Luke, C.M., Cox, P.M.: Excitability in ramped systems: the compost-bomb instability. *Proceedings of the Royal Society A: Mathematical, Physical and Engineering Sciences* **467**(2129), 1243–1269 (2011). DOI 10.1098/rspa.2010.0485. URL <https://royalsocietypublishing.org/doi/10.1098/rspa.2010.0485>
- [36] Wilson, T.A., Beavers, G.S.: Operating modes of the clarinet. *J. Acoust. Soc. Am.* **56**(2), 653–658 (1974)
- [37] Wolfram Research, Inc.: *Mathematica*, Version 13.2. URL <https://www.wolfram.com/mathematica>. Champaign, IL, 2022

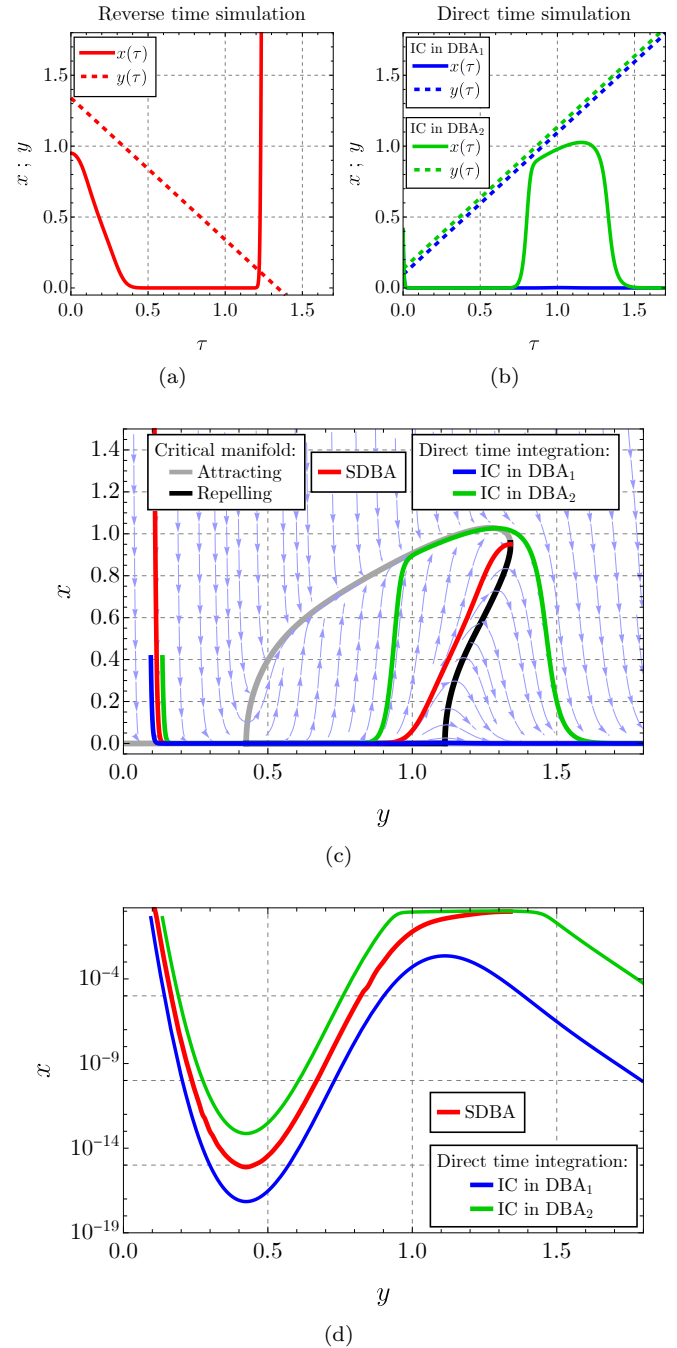


**Figure 3.** Illustration of DBA and SDBA for a linear time-varying blowing pressure. (a) Times series of  $x(\tau)$  (solid line) and  $y(\tau)$  (dashed line) obtained by numerical integration of the reverse time system (15) with  $g(y) = 1$  and an initial condition (IC) given by (16) (red). (b) Time series of the direct time system (4) with a IC first in  $DBA_1$  (in blue) and in  $DBA_2$  (in green). (c) The corresponding orbits (same colors are used) in the phase plane and superimposed to the critical manifold. The orbit corresponding to the reverse time integration corresponds to the SDBA. The stream plot of the vector field Eq. (4) with streamlines colored in light blue is also shown. (d) The same as in (c) but with a logarithmic scale for the ordinates. The parameters are given in Table 1 with in addition  $\epsilon = 0.0183$ .

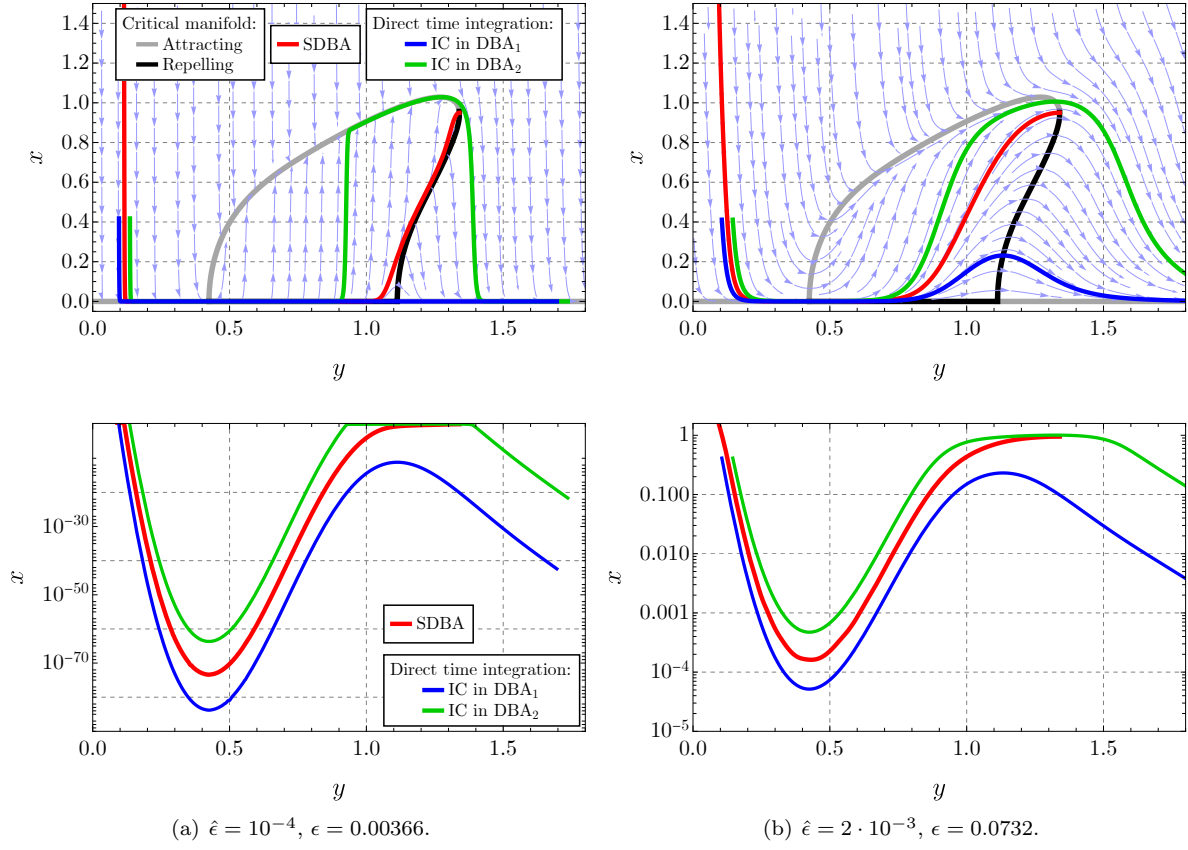


**Figure 4.** The same figures as Figs 3(c) and 3(d) but with (a)  $\hat{\epsilon} = 10^{-4}$  and therefore  $\epsilon = 0.00366$  and (b)  $\hat{\epsilon} = 2 \cdot 10^{-3}$  and therefore  $\epsilon = 0.0732$ .

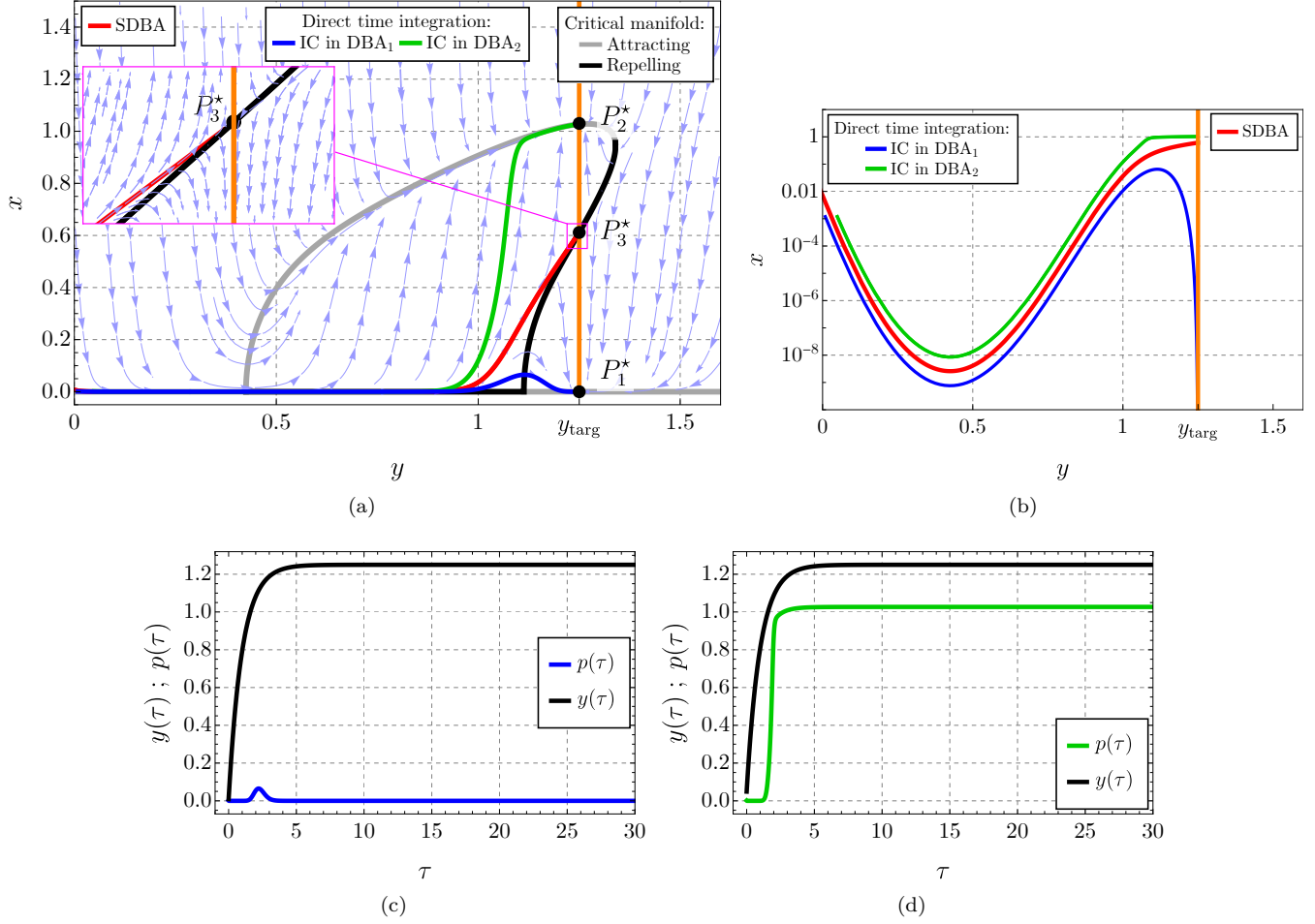


**Figure 5.** Illustration of DBA and SDBA for an exponential time-varying blowing pressure. (a) Orbit obtained by the numerical integration of the reverse time system (15) with  $g(y) = y_{\text{targ}} - y$  and an initial condition (IC) chosen as a small perturbation of the non trivial fixed point  $P_3^*$  (in red). This represents the SDBA of Eq. (18). Two orbits obtained by the numerical integration of direct time system Eq. (18): with a IC first in  $\text{DBA}_1$  (in blue) and in  $\text{DBA}_2$  (in green). The corresponding time series are plotted in Figs. 5(d) and 5(c), respectively. The stream plot of the vector field Eq. (4) with streamlines colored in light blue is also shown. (b) The same as in (a) but with a logarithmic scale for the ordinates. The parameters are given in Table 1 with in addition  $\epsilon = 0.0732$ ,  $y_{\text{targ}} = 1.25$ .

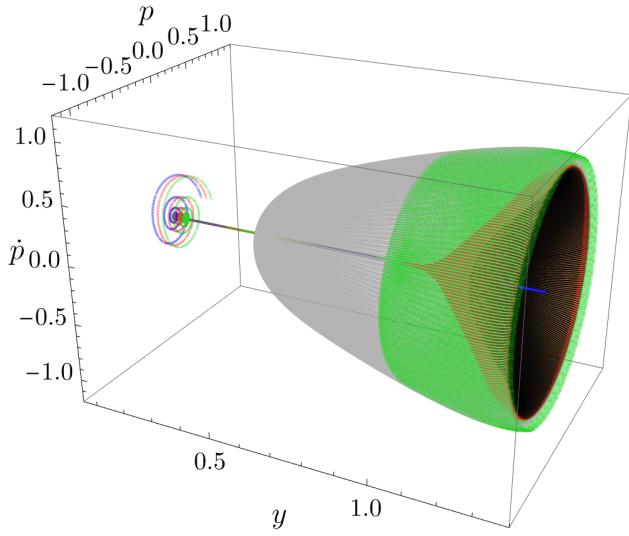


**Figure 6.** Illustration of DBA and SDBA for the original system (27) with a linear time-varying blowing pressure. The manifolds associated to the stable and unstable periodic solutions of the fast subsystem of the original non-averaged dynamics (27) are depicted by gray and black surfaces, respectively. Orbit obtained by the numerical integration of the reverse time system associated to Eq. (27) (replacing  $\gamma$  par  $y(t')$  and switching from  $t'$  to  $t$ , see Appendix A) and an IC on the circle representing the periodic solution in the  $(p, \dot{p})$ -plane at  $y = y_u$  (in red). This represents the SDBA of the 3-dimensional original dynamics. Two orbits obtained by the numerical integration of direct time system: with a IC first in DBA<sub>1</sub> (in blue) and in DBA<sub>2</sub> (in green). Same parameters as in Fig. 3.

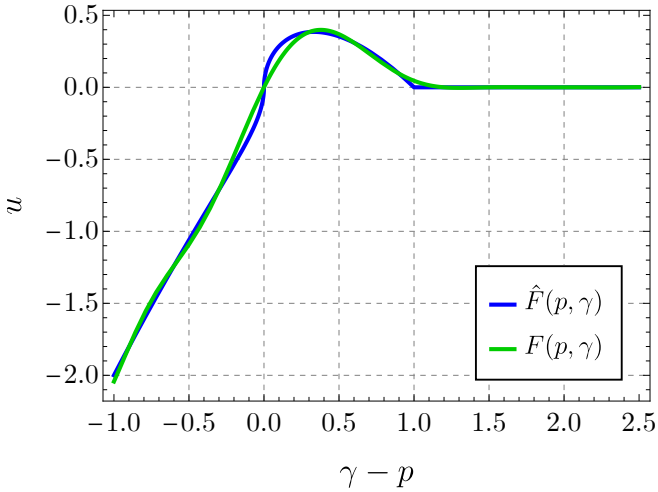


**Figure 7.** Comparison between the function  $\hat{F}(p, \gamma)$  given by Eq. (24) (blue line) and its polynomial fitting  $F(p, \gamma)$  (green line) as functions of the pressure difference  $\gamma - p$ .